Development of design principles for form-fit joints in lightweight frame structures*

C. Weddeling[1], S. Woodward[3], J. Nellesen[2], V. Psyk[1], M. Marré[1], A. Brosius[1], A. E. Tekkaya[1], G. S. Daehn[3], W. Tillmann[2]

[1] Institute of Forming Technology and Lightweight Construction, Technische Universität Dortmund, Dortmund, Germany
[2] Institute of Materials Engineering, Technische Universität Dortmund, Dortmund, Germany
[3] The Ohio State University 2041 College Rd, Columbus, Ohio, USA

Abstract

Based on fundamental technological investigations, alternative joining strategies using electromagnetic forming (EMF) for the flexible production of lightweight frame structures are developed in the collaborative research project SFB/TR10. The results of these investigations will also be used to create general design principles for the joining process itself as well as for the joining zone. The focus of this article will be on dominating form-fit joints of aluminum frame structures and the parameters which have a significant influence on the strength of those joints. For the development of design principles regarding the joining zone, the groove geometry of the connection elements was varied in terms of size and shape, and the influence of those variations was analyzed. In terms of the joining process itself the effect on the joint strength of different forming pressures for a given groove geometry was also investigated. In the first step these experiments were performed on solid mandrels. In order to reduce the weight of the structure, experiments were then performed with hollow connection elements and similar groove geometries to analyze how the reduced stiffness of those elements affected the strength of the joints.

Keywords

Lightweight frame structures, joining, electromagnetic forming

1 Introduction

A current goal of the automotive industry is the reduction of the CO_2 emissions and increase of the fuel efficiency. To achieve this goal, the focus is currently on the

* *This paper is based on investigations of the Transregional Collaborative Research Center SFB/TR10, which is kindly supported by the German Research Foundation (DFG). In the scope of the DFG project INST 212/209-1 FUGG, the high-performance microfocus computer tomography system used in this work could be purchased, which is gratefully acknowledged as well.*

optimization of the powertrain as well as the reduction of a car body's weight. A successful approach to reduce the total weight of a car is the implementation of lightweight strategies in the design process, such as by using light weight materials [1]. The economic production of high strength joints is a major challenge for the manufacturing of a car's frame structure made from extruded aluminum profiles. An interesting alternative to conventional welding and riveting processes is joining by electromagnetic forming since the achievable joint strength is within the range of the strength of the weakest joining partner [2].

2 Fundamentals of joining by electromagnetic compression

2.1 Fundamentals of electromagnetic forming

Electromagnetic forming (EMF) is a noncontact high velocity process using pulsed magnetic fields to deform materials with high electrical conductivity, such as copper and aluminum alloys [3]. Depending on the setup, the tool coil geometry and the work piece, electromagnetic forming can be used for sheet metal forming operations or for the compression as well as the expansion of hollow profiles [4]. The forming process is typically finished after 100 microseconds. This means that a compression speed of 300 m/s can be achieved, which is equivalent to a strain rate of 10^3/s to 10^4/s [5]. A typical setup of work piece, tool coil and forming machine for the electromagnetic compression is shown in Figure 1.

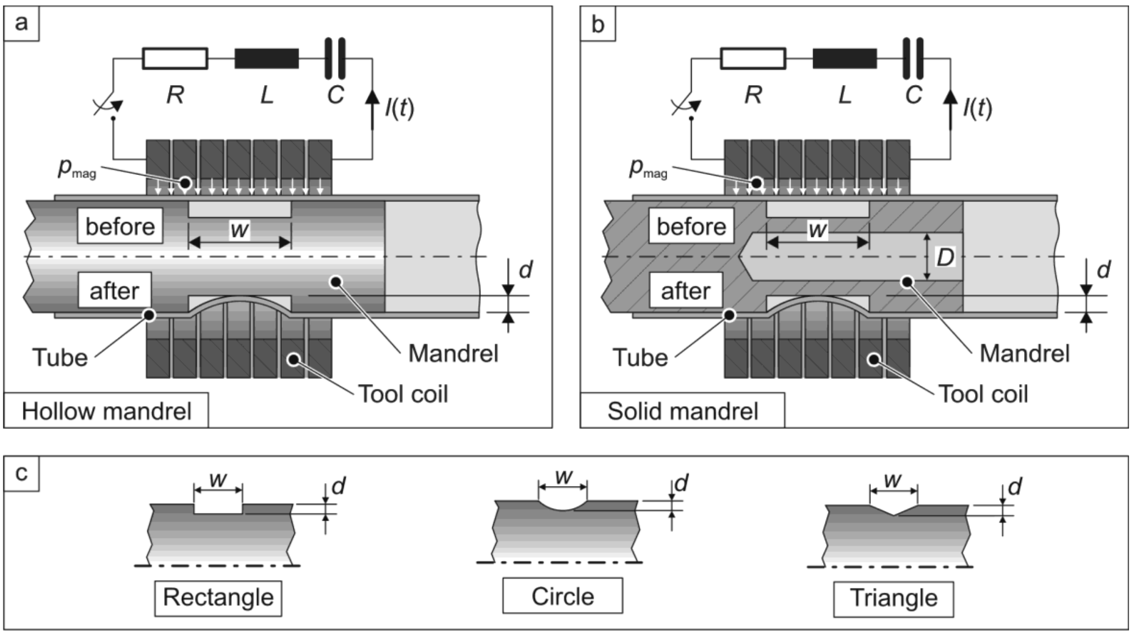

Figure 1 *a) Setup for the experimental investigations on solid mandrels and b) hollow mandrels. c) The different groove shapes (triangle, rectangle, circle) with width w and depth d used within this investigation.*

In the equivalent circuit diagram of this resonance circuit the forming machine is symbolized by the capacitance *C*, the inner resistance R_i and the inner inductance L_i. The work piece and the coil can be seen as a consumer load. Due to a sudden discharge of the electricity stored in the capacitor, a damped sinusoidal current *I(t)* runs through the coil (see Figure 1). The current, which typically ranges from 10 to 1000 kA, generates a magnetic field *H(t,r,z)* around the tool coil. According to Lenz's law, this magnetic field induces eddy currents in the work piece. They are directed opposed to the coil current and they shield the magnetic field from the inside of the work piece. The energy density of the magnetic field represents a pressure *p(t,r,z)* which acts orthogonally on the work piece [4]. Once the stresses in the work piece due to this pressure reach the yield stress of the material, plastic deformation of the tube starts. If the work piece movement is neglected, the magnetic pressure can be calculated by the following equation [6, 7 and 8]:

$$p(t,r,z) = \frac{1}{2}\mu \cdot \left(\frac{n \cdot I(t)}{l_{coil}} \cdot k_H(z)\right)^2 \qquad (1)$$

Within this equation μ represents the permeability, n the number of turns of the coil and l_{coil} the length of the coil. The factor $k_H(z)$ determines the axial distribution of the magnetic field [9].

2.2 Joining by electromagnetic compression

Joining of tubular work pieces by electromagnetic compression is the most frequently used EMF application. The manufacturing of those joints does not require additional joining elements, such as screws, rivets, adhesives or auxiliary wire. According to the most dominating mechanism against an external load, joints manufactured by electromagnetic forming can be classified into interference-fit joints, form-fit joints and welded joints. Interference-fits are manufactured by a plastic deformation of one and an elastic deformation of the other joining partner so that interference stresses result [2]. For a form-fit joint, the material of one joining partner is formed into an undercut (e.g. a groove) of the other joining partner (see Figure 1). As a result, the joint is locked against an external load. In the case of very high impact velocities of the electromagnetically driven part it is possible to produce welded bonds between the joining partners. This application is called magnetic pulse welding. Furthermore, the resistance against an external load can be a result of a combination of each of those mechanisms. Typically, the loads which can be transferred by a dominating form-fit or welded connection are higher than those which can be transferred by an interference-fit joint. Compared to form- and interference-fit joints, welded connections usually require a much higher energy to be manufactured. Since similar joint strengths can be achieved by form-fit as with magnetic pulse welded connections, this kind of joint shall be investigated in the following. The factors which influence the strength of a connection formed by electromagnetic compression shall be analyzed.

Very detailed studies on the influence of different groove parameters on the joint strength of form-fit connections were done by Bühler [10 and 11], Golovashchenko [12] and Park [13]. In their work Bühler and Golovashchenko investigate the influence of the groove width *w* and depth *d* on the achievable joint strength for electromagnetically compressed form-fit joints. For their investigation, they varied the acting magnetic pressure in such a way that the tube wall just touched the groove base. They found that an increase of the groove depth as well as a decrease of the groove width lead to higher joint strengths. In contrast to Bühler and Golovashchenko, Park used a constant forming pressure in his work. He also found an increase in the joint strength with an increase of the groove depth. But he observed an increase of the joint strength with an increase of the groove width. This can be explained by the constant forming pressure Park used in his experiments. The pressure required to form a tube into a groove so that its wall just touches the groove base decreases with increasing groove width. This is a result of the lower stiffness of the tube wall covering the groove [11]. Therefore, a constant forming pressure leads to an enlarged contact area at the groove base for wider grooves. As a result of the compressive forming, residual hoop stresses are generated in the contact area. Due to these stresses, an interference-fit is generated, and its effect on the overall joint strength grows with an increase of the contact area and therefore with wider grooves [13]. Park also investigated the influence of the groove edge radius on the joint strength. He found that up to a certain point a smaller edge radius leads to higher joint strength. But a decrease of the radius also causes an increase of shearing at the groove edge. As a result of these opposing effects, an optimal groove edge radius exists for a given groove depth [13]. All three research works also showed that the strength of a form-fit connection can be increased significantly by using multiple grooves.

3 Motivation

The results of the previous studies introduced above were applied for the design of form-fit joints for the lightweight frame structure shown in Figure 2 b). But the resulting joint strengths were much lower than expected from those studies. For weight reduction purposes, the inner joining partners were designed as hollow aluminum parts, which led to a much lower stiffness than the mandrels used by Bühler, Golovashchenko and Park for their experiments.

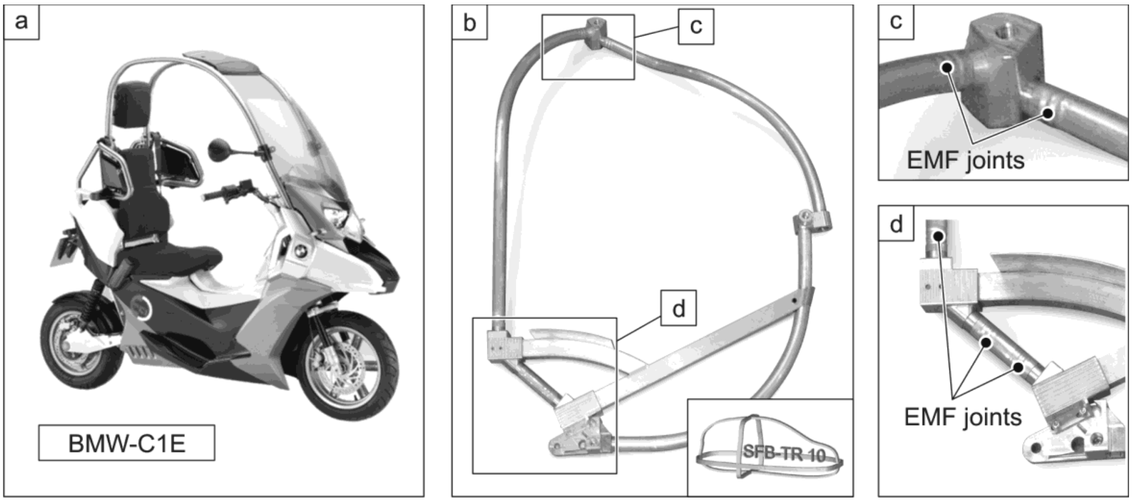

***Figure 2** a) BMW-C1E. b) Alternative frame structure for the BMW-C1E manufactured within the collaborative research center SFB/TR10. c) and d) EMF form-fit joints*

To determine the reason for the significant drop in joint strength and to develop joining strategies for those lightweight frame components, an investigation was carried out, the results of which are presented in the following. This development of joining strategies includes a study regarding the influence of different groove shapes on the joint strength. This parameter is especially important in terms of corrosion aspects. In case of a rectangular groove design, cavities are generated at the groove edges. These cavities are potential starting points of corrosion. By using circular grooves, these hollow spaces can be avoided. But this groove shape might lead to a different joint strength than the rectangular groove geometry.

4 Experimental investigation of the joining zone characteristics on the joint strength

Fundamental experiments were performed to indentify the parameters which affect the strength of form-fit joints for lightweight frame structures. The basic setup of the experiments carried out within this work is displayed in Figure 1 a) and b). For the experiments, solid and hollow mandrels with an outer diameter of 36 mm were used. The charging energy during the joining experiments was adjusted in order to apply the minimum amount of magnetic pressure that was required to cause contact between the tube and the bottom of the groove. This was defined as “filling” the groove, similar to the approaches of Bühler and Golovashchenko [10, 11 and 12]. The drilled hole in the hollow inner joining partners had a diameter of 24 mm. This diameter was chosen to ensure that, for all groove depths, the smallest annulus area of the mandrel was bigger than the annulus area of the tube. As a result, the tube was always the weaker joining partner. For the investigation of the influence of the groove shape, rectangular, circular and triangular grooves were machined into the mandrels (see Figure 1 c)). These grooves had three different widths *w* (12, 16 and 20 mm) as well as three different depths *d* (1, 1.5 and 3 mm). This variation was done to obtain a complete understanding of the parameters influencing the joint strength. To minimize an additional possible interference-fit between the joining partners, the same material, namely EN AW-6060 (F22), was chosen for the tubes and the mandrels [14]. For the same reason, there was no gap between the joining partners. The outer diameter of the tubes was 40 mm and the wall thickness 2 mm. To generate the magnetic pressure pulses, a Maxwell Magneform machine (Series 7000) was used. The relevant machine parameters were a capacitance *C* of 362 µF, an inductance L_i of 78 µH and an inner resistance R_i of 5.4 mΩ. As EMF actuator, a compression coil with an inner diameter of 40 mm and 10 turns distributed over a coil length of 60 mm was used.

4.1 Determination of the forming pressure

As mentioned above the forming pressure was selected in dependence on the groove dimensions width and depth. To find the proper forming pressure an analytical-experimental approach was used. In the first step the pressure p_{min} required to initiate the plastic deformation of the tube into the groove was determined. Therefore, the following equation developed by Bühler was used [11]:

$$p_{min} = \sigma_y \left[3 \cdot \left(\frac{s}{w}\right)^2 + \frac{s}{R}\right] \quad (2)$$

Within this equation σ_y represents the yield stress of the tube material, *s* the wall thickness and *R* the outer radius of the tube. The groove width is represented by *w*. The result of this analytical model provided an approximate starting point for the second step in the approach (see Figure 3). To determine the exact pressure required to fill a groove of any desired dimensions experimental data were used. The objective of these experiments was to determine the correlation between magnetic pressure and the resulting depth of forming into the channel. For these tests, two greased steel cylinders were inserted into an aluminum tube. They were connected by a threaded rod to adjust their distance. The cylinder gap width *w* was matched with the three groove widths for the mandrels: 12, 16, and 20 mm. The tubes were then electromagnetically formed into the gap between the steel cylinders using charging energies between 2.4 kJ and 6 kJ, at intervals of 1.2 kJ.

The measured discharge currents varied between 55 kA for 2.4 kJ and 90 kA for 6 kJ of charging energy. The rise time of the discharge was approximately 22 µs. After the removal of the cylinders, a ZEISS PRISMO VAST 5 HTG coordinate measurement machine was used to determine the maximum forming depth *d*. Figure 3 shows the resulting depth versus the respective magnetic forming pressures. The calculation of these pressures was based on the applied discharge current, using Equation 1. Upon plotting the magnetic pressures versus forming depths it could be seen that, for each gap width *w*, the resulting forming depth *d* rises linearly with the applied magnetic pressure. Figure 3 also shows that increased forming depths or decreased gap widths require a higher forming pressure.

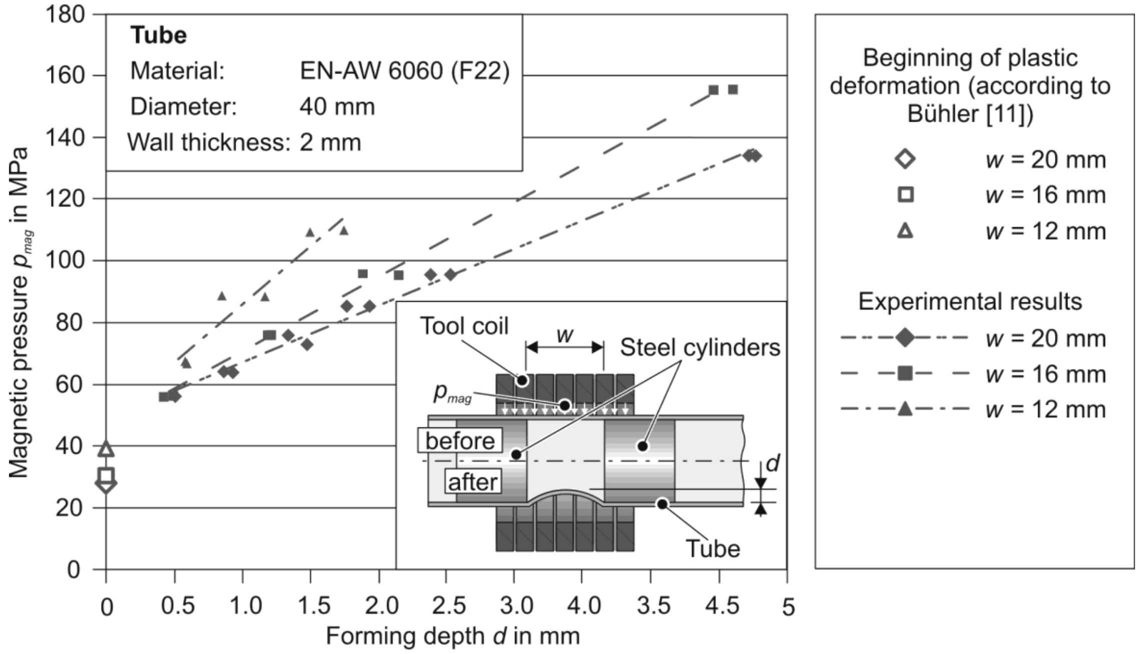

Figure 3 *Influence of the magnetic pressure on the achieved forming depth d for different groove widths w.*

By substituting a specific groove depth into the equation of the corresponding trend-line, the required magnetic pressure to fill a groove can be determined with a high degree of accuracy. The calculated pressure for each parameter set was multiplied by a safety factor of 1.1 to ensure filling. This factor accounts for the differences between the steel cylinders in the pre-tests and the aluminum mandrels used to create the joints. It also accounts for any possible inhomogeneities in the tube material.

4.2 Influence of the groove dimensions and shape on the joint strength

In order to analyze if the determined magnetic pressures were accurate and the tube wall touches the groove base, X-ray radioscopy and micro computer-tomography measurements were performed after the joining process. Another reason for these studies was to detect a possible shearing or thinning of the tube wall at the groove edges. A high-performance computer tomography system equipped with two X-ray tubes (directional microfocus and tube with transmission target) was used to carry out those measurements. The machine is equipped with a 7-axis manipulator and a large-sized flat-panel detector with an active area of 409.6 x 409.6 mm², containing 2048 x 2048 square pixels (see

Figure 4 a)). The X-rays which are emitted from the focal spot on the target of the microfocus tube penetrate the specimen and are attenuated due to interaction processes with matter. Since the X-rays diverge, the specimen is projected onto the detector plane with a magnification given by the ratio between the focus-detector-distance and the focus-object distance. Figure 4 shows the specific parameters which were used for the non-destructive 2D inspection and tomography. The joint of the specimen was mapped with maximum magnification onto the detector plane. This resulted in a reconstructed tomogram containing roughly 2000 x 2000 x 1000 voxels with a voxel edge length of 22 µm. An algorithm developed by Feldkamp [15] was used for the reconstruction.

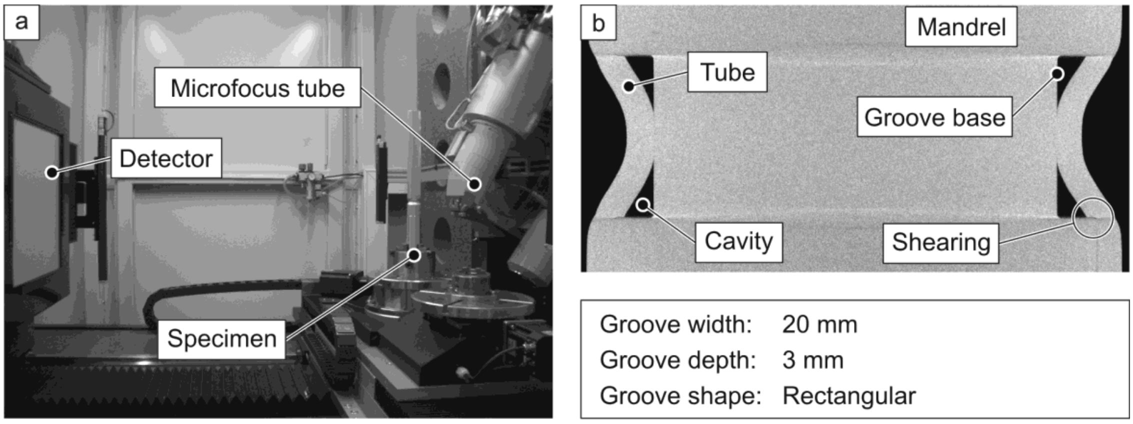

Groove width:	20 mm
Groove depth:	3 mm
Groove shape:	Rectangular

Computertomography (CT) Parameters

Acceleration voltage U_B:	230 kV	Magnification *m*:	~ 9.2
Tube current *I*:	100 µA (120 µA)	Geometry:	Cone Beam
Prefilter:	0.5 mm Cu	Number of Angular Position:	2200 (1440)
Focus-Object-Distance *FOD*:	131 mm	Angle Increment:	~ 0.164° (~ 0.25°)
Focus-Detector-Distance *FDD*:	1200 mm		

( ) = if parameters varied for the hollow mandrels

Figure 4 *a) Setup of the radioscopic and computer tomography (CT) measurements. b) CT image of a form-fit joint with a rectangular groove of 20 mm width and 3 mm depth.*

In Figure 4 c) a xy-slice of the joining zone is displayed. It can be seen that the tube wall makes contact with the groove. The tube wall lies against the deepest point of the groove (groove base) but cavities above and below the plane containing the groove base can also be observed. To determine the quality of the generated joints, pull-out test were performed afterwards. For these experiments a universal testing machine Zwick SMZ250 was used. A pull-out rate of 0.05 mm/s was chosen. Figure 5 a) shows a typical pull-out curve which was obtained by these tests. The force F_J was defined as failure criterion of the connections. At this force, the first relative movement between the tube and the mandrel occurred. Its value was indicated by a change in slope of the load-extension curve (see Figure 5 a)). This criterion was chosen in accordance with the work of Bühler [10]. In Figure 5 b) the two different failure modes which were observed during tensile testing are displayed: pull-out of the tube from the groove and tearing of the tube at the leading groove edge. Both failures occurred shortly after the connections reached their ultimate pull-out force. The tearing of the tube was observed when higher forming energies were applied to deeper and/or narrower grooves. This could be attributed to the tube being partially sheared at the groove edges as it was formed into the grooves at higher magnetic pressures. For these joints the F_J as well as the ultimate pull-out force was higher than for those connections which failed by pull-out of the tube. Furthermore, the joints failing by tearing of the tube failed more suddenly due to a lower plastic deformation of the connection before the final separation of the joining partners.

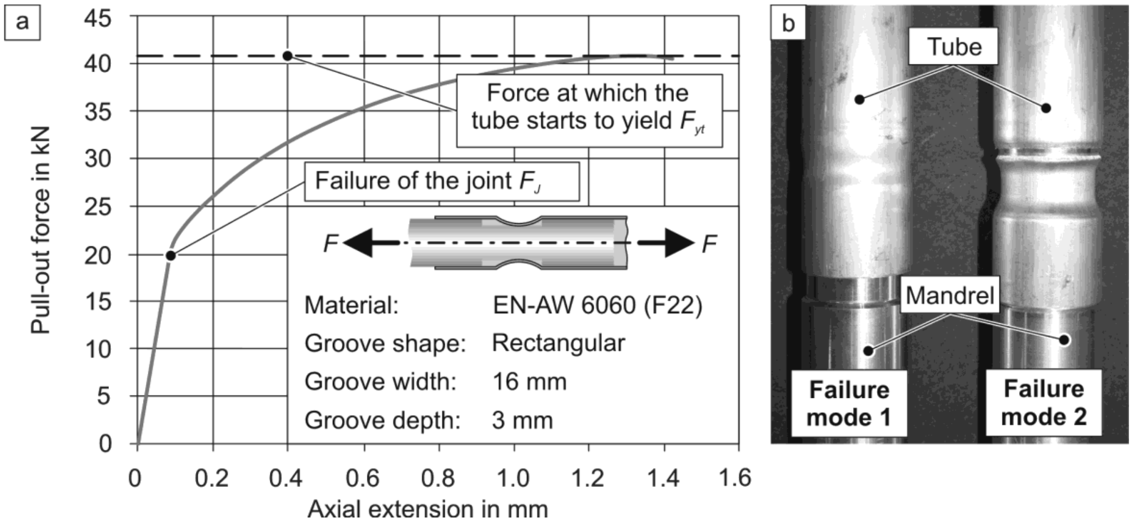

Figure 5 *a) Typical pull-out curve of the joint specimens. b) The two failure modes observed within this work: pull-out (left) and tearing (right) of the tube.*

The forces at which the joints failed were plotted versus the groove depth for different groove width and shapes (see Figure 6 a) and b)). The values of F_J were normalized with respect to the yield force of the tube itself, F_{yt}. Figure 6 a) shows that an increase of the groove depth as well as a decrease of the groove width leads to an increase in joint strength.

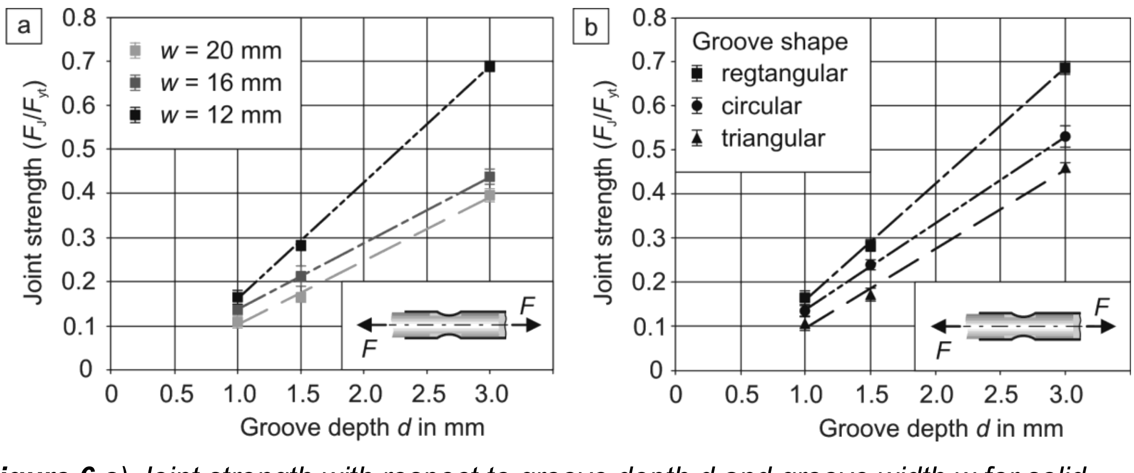

Figure 6 *a) Joint strength with respect to groove depth d and groove width w for solid mandrels with a rectangular groove shape. b) Joint strength with respect to groove depth d and different groove shapes for 12 mm wide grooves.*

This could be attributed to the fact that the resulting angle α (see Figure 7 b)) decreases with deeper or narrower grooves, which increases the incremental degree of deformation at the groove edge and thus requires a larger pull-out force. For all three grooves, the distribution of the data points suggested a linear relationship between the depth of the groove and the pull-out. An upper limit of this linear relationship is expected due to the partial shearing of the tube at the groove edge, as shown in Figure 7 b). Eventually, the thinning of the tube due to shearing at the groove edge will weaken the joint more than the strength increase observed when forming the tube into a deeper/narrower groove, causing the overall joint strength to decrease. In the next step of this study the influence of the groove shape on the connection strength was analyzed. Figure 6 b) shows the normalized pull-out forces with respect to the depth of the groove for a constant groove width of 12 mm. For each groove shape, the point distributions again show a linear relationship between groove depth and pull-out force. Figure 6 b) shows that, for each individual groove depth, the joints formed with rectangular grooves always exhibit the highest joint strength, while the joints formed with triangular grooves are always the weakest.

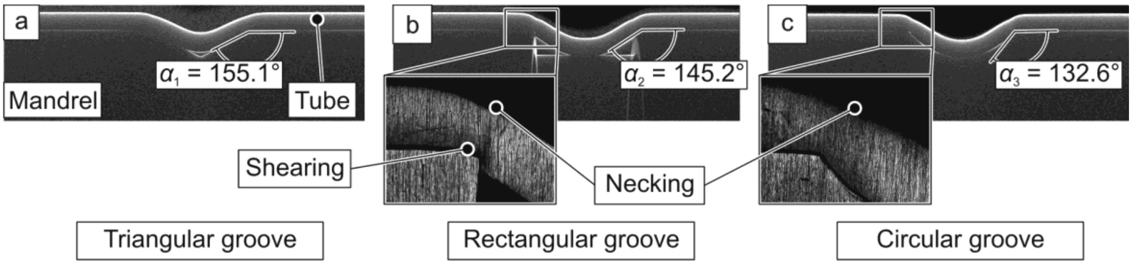

Figure 7 *Measurement of the angle α at the groove edge in radioscopic pictures of 3 mm deep and 12 mm wide grooves with different groove shapes.*

This could be attributed to the fact that the resulting angle *α* of the tube wall at the edge of the triangular geometry is greater than those of either the circular or rectangular grooves (see Figure 7). Therefore, the degree of deformation at the edge of the groove is lower and a smaller tensile force is required to initiate pull-out. Although Figure 7 displays that the joints generated with circular grooves have a smaller resulting angle *α* than the joints formed with rectangular grooves, the use of rectangular grooves results in a larger pull-out force for each parameter set. This can be explained by the fact that the amount of shearing at the groove edge is higher for the rectangular grooves than for the circular ones (compare Figure 7 b) and c)). Due to the greater partial shearing, the rectangular groove locks the tube in place more firmly than when formed into the circular groove, and thus requires a greater pull-out force. This is further supported by the fact that, as Figure 6 b) shows, the use of mandrels with rectangular grooves causes failure by tearing at the leading groove edge for groove depths of both 1.5 and 3 mm, whereas the failure of the connections with circular grooves was caused by tearing of the tube only for the 3 mm deep grooves. The fact that joints with rectangular grooves exhibit this failure mode at a shallower groove depth suggests that the effects of shearing play a more prominent role in the strength of this groove geometry, and it is possible that this accounts for the larger required pull-out forces.

4.3 Effects on the strength of joints with hollow inner joining partners

As mentioned above, the reduction of weight is a very important goal for the automotive industry, which means that the frame structure of a vehicle has to be as light as possible. Therefore, the joining behavior and the achievable joint strength for connection including hollow inner joining elements were also investigated. Figure 8 a) shows the achieved joint strength for different groove depths with respect to the width of the grooves. The results in terms of the relationship between connection strength and groove depth/width are similar to the experimental findings for the solid mandrels. But especially the grooves with a width of 12 mm showed a significant drop in strength of up to 20% compared to joints which were formed onto solid mandrels with equivalent groove geometry. This could be attributed to a significant deformation of the mandrel, which is shown by the tomography image in Figure 8 b). This deformation led to an increase of the angle α at the groove edge. As described above, this decreases the incremental degree of deformation at the groove edge and thus requires a lower pull-out force. Due to the deformation of the mandrel the tube wall also did not touch the groove base. As a result, there was no interference-fit generated in this area. Whereas, without a deformation of the mandrel, this additional interference-fit would occur because, during forming, the plastic deformation in the tube creates a small amount of elastic deformation in the mandrel.

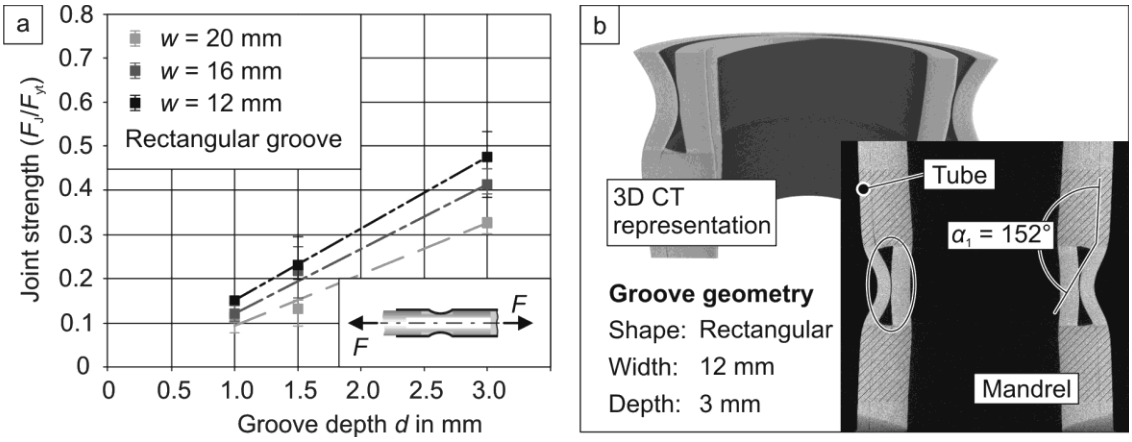

***Figure 8** a) Joint strength with respect to groove depth d and groove width w for hollow mandrels. b) Form-fit joint with a hollow mandrel as inner joining partner; upper left: 3D representation of the tomogram of the joint; lower right: 2D CT image (yz-slice) of the joint.*

When the forming process ends, the mandrel would be unable to release this elastically stored energy due to the plastic deformation in the tube, which would result in interference stresses at the contact surface between the tube and mandrel. This interference stress would resist tube pull-out during tensile testing, thereby increasing joint strength. Although there was no interference-fit generated at the bottom of the groove, an interference-fit was produced at the areas next to the groove (see hatching in 2D CT image Figure 8 b)). Since the same material was used for both joining partners, the additional joint strength created by this interference-fit was too low to compensate the losses due to the weaker form-fit joint [14]. The joints with a groove width of 16 or 20 mm showed only a very small deformation of the mandrel. This explains why they had almost the same joint strength as connections with equivalent groove geometry and solid mandrels. The larger deformation of the mandrels with a groove width of 12 mm resulted from the higher magnetic pressure used to generate these joints compared to those with wider grooves and an equivalent depth (see Figure 3).

A strategy to avoid the deformation of the inner joining partner and the resulting drop in joint strength is the usage of a support mandrel which is placed in the hole of the mandrel during the joining process. Since this support tool shall be removed after the joining process, an interference-fit between the mandrel and the support element has to be avoided. Therefore, a material which has a lower elastic recovery than the mandrel has to be used for the support tool. This can be achieved by using a material with a higher Young's modulus or a lower yield stress than the mandrel material [14]. Within this study, a steel support mandrel with a Young's modulus three times higher than EN AW-6060 was used. Figure 9 a) shows the achieved pull-out strength for the connections formed with a support element compared to the strength of those which were joint without a support tool. It was possible to increase the joint strength with this setup significantly. The achieved increase was about 15% which means that the pull-out strength level of the joints with solid mandrels was almost reached. Figure 9 b) shows that the deformation of the inner joining partner was reduced significantly which led to the observed increase in joint strength.

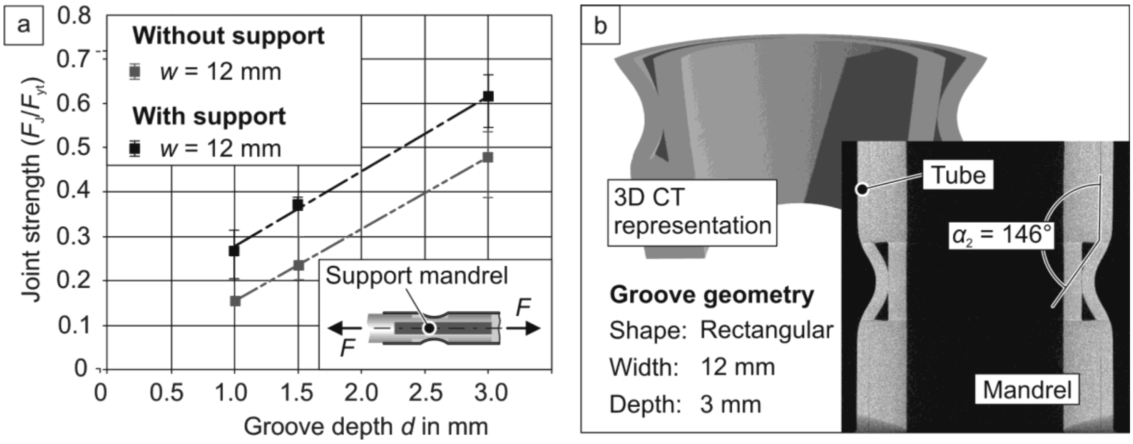

Figure 9 *a) Comparisons of the achieved pull-out strength between a joint generated with and one without the usage of a support mandrel. b) Form-fit joint which was supported by a stainless steel mandrel during the joining process; upper left: 3D representation of the tomogram of the joint; lower right: 2D CT image (yz-slice) of the joint.*

5 Conclusion

The results of this work have shown that the joining of extruded aluminum profiles by electromagnetic compression is a feasible approach to create lightweight frame structures. Due to a decrease of the angle α at the groove edge and the resulting increase of the degree of deformation during pull-out at this edge, the joint strength increases with deeper and narrower grooves. The results of the experimental investigations also showed a significant influence of the groove shape on the achievable joint strength. The highest connection strengths were observed for the rectangular grooves due to the presence of partial tube shearing at the groove edges. This shearing locked the tubes into place, requiring a larger pull-out force to cause failure. Although the partial shearing of the groove edge increased the quasi-static strength of the joints, it can be assumed that it is very problematic for connections which are exposed to cycling loads. Since the location of the shearing is a starting point for the formation of a crack, it has to be avoided for joints under cycling loads. It can be assumed that a rounded groove edge would reduce the formation of such a crack. But further investigations are necessary to determine the precise influence of the groove edge radius on the joint failure and the transferable loads.

The joining experiments with hollow inner joining partners have shown that the applied forming pressure in relation to the stiffness of the mandrel has a significant influence on the achievable joint strength. If the magnetic pressure required to "fill" the groove exceeds the stiffness of the inner joining partner, a deformation of this element occurs. As a result the angle α at the groove edge is increased, which will lead to a decrease in joint strength. Therefore, it is important to consider the mandrel's stiffness with respect to the applied pressure during the design process of the joining elements. The deformation of the mandrel can also be avoided by using a support mandrel during the joining process. By placing this additional tool in the hole of the inner joining partner it was possible to achieve pull-out strengths similar to those achieved for connections with solid mandrels.

References

[1] Kleiner, M., Geiger, M., Klaus, A.: Manufacturing of Lightweight Components by Metal Forming. Annals of the CIRP "Manufacturing Technology". 53rd General Assembly of CIRP Vol. 52, Issue 2 (2003). Montreal, Canada, pp. 521 – 542.

[2] Marré, M., Brosius, A., Tekkaya, A. E.: Joining by Compression and Expansion of (None-) Reinforced Profiles. Advanced Materials Research: Flexible Manufacture of Lightweight Frame Structures - Phase II: Integration, Vol. 43. (2008), pp. 57 – 68.

[3] Daehn, G. S.: High-Velocity Metal Forming. ASM Handbook Vol. 14B, Metalworking: Sheet Forming. ASM International (2006), pp. 405 – 418, ISBN 0-87170-710-1.

[4] Bruno, E. J.: High Velocity Forming of Metals. Dearborn, Michigan, ASTME (1968).

[5] Weimar, G.: Hochgeschwindigkeitsbearbeitung III Umformung von Blechen und Rohren durch magnetische Kräfte. Werkstatt und Betrieb Vol. 96, Issue 12 (1963), pp. 893 – 900.

[6] Winkler, R.: Hochgeschwindigkeitsbearbeitung. VEB Verlag Technik, Berlin (1973).

[7] Mühlbauer, A., von Finckenstein, E.: Magnetumformung rohrförmiger Werkstücke. Bänder Bleche Rohre Vol. 8, Issue 2 (1967), pp. 86 – 92.

[8] Kleiner, M., Beerwald, C., Homberg, W.: Analysis of Process Parameters and Forming Mechanisms within the Electromagnetic Forming Process. CIRP Annals – Manufacturing Technology Vol. 54, Issue 1 (2005), pp. 225 – 228.

[9] Beerwald, C.: Fundamentals for Process Dimensioning and Design of Electromagnetic Forming (in German). Dr.-Ing. Thesis, Universität Dortmund (2004).

[10] Bühler, H., v. Finckenstein, E.: Fügen durch Magnetumformung. Werkstatt und Betrieb 101 (1968), pp. 671 – 675.

[11] Bühler, H., v. Finckenstein, E.: Bemessung von Sickenverbindungen für ein Fügen durch Magnetumformung. Werkstatt und Betrieb 104 (1971), pp. 45 – 51.

[12] Golovashchenko, S.: Methodology of Design of Pulsed Electromagnetic Joining of Tubes. Proceedings of the TMS Symposium "Innovations in Processing and Manufacturing of Sheet Materials". New Orleans, Louisiana, United States of America (2001), pp. 283 – 299.

[13] Park, Y., Kim, H., Oh, S.: Design of axial/torque joint made by electromagnetic forming. Thin-Walled Structures Vol. 43 (2005), pp. 826 – 844.

[14] Marré, M.: Grundlagen der Prozessgestaltung für das Fügen durch Weiten mit Innenhochdruck. Dr.-Ing. Thesis, Technische Universität Dortmund (2009), Shaker Verlag Aachen, ISBN: 978-3-8322-8361-2.

[15] Feldkamp, L. A., Davis, L. C., Kress, J. W.: Practical cone-beam algorithm. Journal of the Optical Society of America Vol. 1, Issue 6 (1984), pp. 612 – 619.